Model for the Sulfidation of Calcined Limestone and Its Use in Reactor Models

A. B. M. (Bert) Heesink, D. W. F. (Wim) Brilman, and W. P. M. (Wim) van Swaaij
Dept. of Chemical Engineering, Twente University of Technology, 7500 AE Enschede, The Netherlands

A mathematical model describing the sulfidation of a single calcined limestone particle was developed and experimentally verified. This model, which includes no fitting parameters, assumes a calcined limestone particle to consist of spherical grains of various sizes that react with H_2S according to the classic shrinking-core model. The initial size distribution of the grains is derived from mercury porosimetry. The transport of H_2S through the bidisperse limestone particle is calculated based on the random-pore model of Wakao and Smith, which distinguishes macropore and micropore zones. Knudsen diffusivity inside the micropore zones is calculated according to the dusty-gas approach. The single-particle model delivers the value of a new defined utilization factor, which includes effects of external mass-transfer limitation, pore-diffusion limitation, and grain-size distribution on particle reactivity. A correlation derived for a single batch of calcined limestone explicitly expresses this utilization factor as a function of conversion and relevant process parameters. This correlation can be easily incorporated into reactor models, as shown for an existing model describing the capture of H_2S by a fluidized bed of calcined limestone particles.

Introduction

Limestone, both in raw and in calcined form, can be used to remove H_2S from coal gas. Whereas calcined limestone can be fully utilized, the absorption capacity of uncalcined limestone is no more than 10% (Fenouil and Lynn, 1995a; Illerup et al., 1993). Therefore, calcined limestone is the more attractive sorbent for nonregenerative coal-gas desulfurization. The kinetics of the reaction between H_2S and calcined limestone (i.e., $CaO + H_2S \rightarrow CaS + H_2O$) have been examined by, for example, Allen and Hayhurst (1990), Fenouil and Lynn (1995b), and Heesink and Van Swaaij (1995a). All investigators reported reaction rates being high enough to allow the use of calcined limestone for coal-gas desulfurization on a practical scale.

In order to describe sulfidation in the kinetically controlled regime, Heesink et al. (1993) developed the so-called grain-size distribution (GSD) model. This model is based on the grain model first proposed by Szekely and Evans (1970), but additionally takes the size distribution of the reacting grains into account, which is quite relevant, as was shown by Szekely and Propster (1975). By doing so, the GSD model has proven to predict the sulfidation of calcined limestone quite well, provided that the rate of reaction is controlled by intrinsic kinetics. In practice, though, the rate of sulfidation may well be limited by the mass transfer of H_2S. Therefore, in this article, a new model is presented that predicts the sulfidation of a single limestone particle under all conditions, including those where mass-transfer limitation occurs. This combined pore and grain-size distribution (or CPGSD) model is based on the GSD model and the random-pore model of Wakao and Smith (1962).

Many mathematical models that describe the conversion of a solid particle by a reactant gas at conditions where mass-transfer phenomena play a role have already been developed. All models in some way describe the change in diffusivity inside the reacting particles when the molar volumes of the solid reactant and the solid product are different and the internal structure of the particles changes (resulting in, e.g., pore plugging). Models describing the sulfation of a single calcined limestone particle by SO_2 were developed by Hartman and Coughlin (1976), Ramachandran and Smith (1977), and Bhatia and Perlmutter (1981), to name a few, and, more recently, by Brem (1990) and Dam-Johansen et al. (1991). The

Correspondence concerning this article should be addressed to A. B. M. Heesink.

sulfidation of zinc oxide was modeled by Ranade and Harrison (1981), Lew et al. (1992), and Efthimiadis and Sotirchos (1993a,b). Some models were developed that predict the conversion of particles undergoing structural changes not only due to chemical reaction but also to simultaneous sintering (Ranade and Harrison, 1981; Alvfors and Svedberg, 1992). More recently, Zevenhoven et al. (1996) developed a model to describe the capture of H_2S by limestone and dolomite.

A new model presented here differs from previous ones in one or more of the following ways:

- It takes the measurable grain-size distribution into account and describes the structure of the porous particles without the use of any fitting parameters.
- It uses the grain concept to describe diffusivity as a function of particle conversion by application of the dusty-gas approach, regarding the grains as large immobile dust molecules (see also Dam-Johansen et al., 1991).
- It can handle any reaction order in gaseous reactant (though it assumes that the reaction order does not vary with gas concentration as in the case of, for example, Langmuir–Hinshelwood kinetics).
- Through the introduction of a new-defined utilization factor it offers a means to apply the single-particle model in reactor models. Like the model presented in this article, many single-particle models are too complex for simple inclusion in a reactor model. For that reason simplified semiempirical single particle models have been developed; for example, by Schouten and Van den Bleek (1987) and later Lin (1994) to describe the capture of SO_2 by limestone in fluidized-bed coal combustors. The utilization factor, as defined in this article, can be used to apply the results of the much more comprehensive CPGSD model in reactor models, describing the capture of H_2S by calcined limestone in a gas–solid contactor.

We will first discuss the basis of the presented CPGSD model and define a new utilization factor. Next, the model will be experimentally verified by comparing measured and simulated conversion behavior of calcined limestone particles when these are sulfided in a thermogravimetric analyzer. Then, for a single type of calcined limestone, it will be examined how the utilization factor depends on different process-related parameters. It will be shown that the utilization factor can be explicitly expressed as a function of these parameters by means of a simple correlation. Finally, this correlation is implemented in an existing reactor model that predicts the capture of H_2S in a bubbling fluidized-bed absorber containing calcined limestone particles. Predicted capture will be compared with the capture measured with a small fluidized-bed absorber, in which H_2S is removed from simulated coal gas by a batch of calcined limestone particles.

Single Particle Model

According to the GSD model of Heesink et al. (1993), a calcined limestone particle is presumed to be a collection of spherical grains of various sizes. This concept is illustrated in Figure 1. The radii of the grains depend on calcination conditions and may range from 10 nm to 500 nm. Since calcined limestone has a bidisperse nature (Nguyen and Watkinson, 1993), distinction is made between micropore zones and macropores. The grains are gathered together in clusters that constitute the micropore zones. These zones are separated

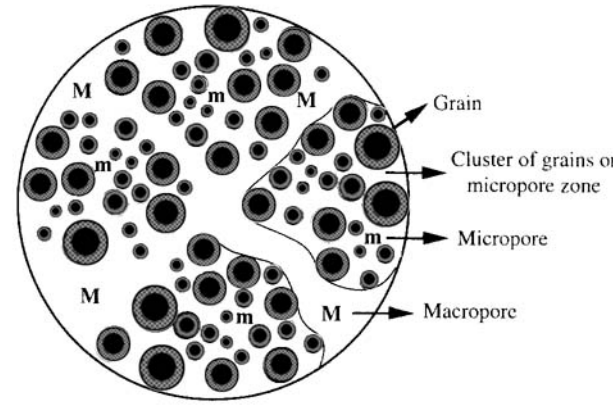

Figure 1. Calcined limestone particle according to the grain model of Szekely and Evans (1970).

from each other by macropores that have a radius of 0.1 to 3 μm (Borgwardt and Harvey, 1972; Hartman et al., 1978). The size of the individual grains is derived from the pore-size distribution as measured by, for example, mercury porosimetry. The ratio of the radii of a grain and its surrounding pores is referred to as "pore-to-sphere factor" (F). The value of this ratio does not depend on pore (or grain) size and can be obtained from mercury porosimetry. For example, Figure 2 shows a porosigram of calcined limestone from the quarry at Wülfrath (Germany). The porosigram is divided into a number (N) of pore-size intervals. Because reactivity is proportional to the amount of specific surface area involved, only that part of the porosigram that represents a substantial surface area is considered. In the case of Figure 2, pores having a radius larger than about 100 nm (representing only a minor part of the total specific surface area) are neglected. These macropores are located in between clusters of grains and not in between individual grains. The size of the grains surrounded by pores belonging to size class i, follows from

$$R_{o,i} = F \cdot R_{p,i}. \tag{1}$$

The common volume of the pores belonging to size interval i ($V_{p,i}$) is a measure of the common weight of grains with ra-

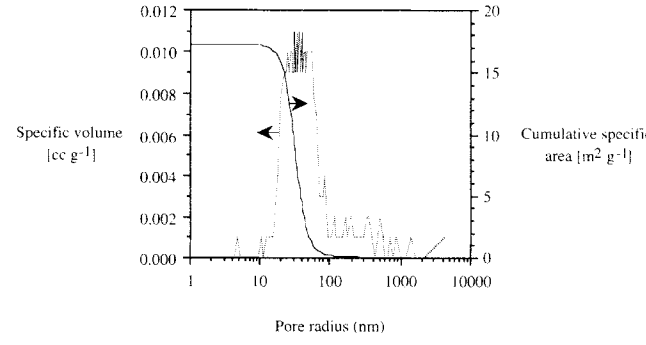

Figure 2. Porosigram of Wülfrath limestone calcined in a fluidized-bed reactor by heating to 850°C while purging with N_2.

$N = 5$: $\nu_1, \ldots, \nu_5 = 0.17, 0.35, 0.32, 0.12, 0.04$; $R_{p,1}, \ldots, R_{p,5} = 21, 30, 40, 53, 78$ nm; $F = 1.56$.

dius $R_{o,i}$. The weight fraction of the grains belonging to size class i (ν_i) can thus be calculated from

$$\nu_i = \frac{V_{p,i}}{\sum_{j=1}^{j=N} V_{p,j}}. \tag{2}$$

The specific surface area A of a mixture of different-size spheres by definition equals

$$A = \frac{3}{\rho_{\text{sol,reac}}} \sum_{i=1}^{i=N} \frac{\nu_i}{R_{o,i}}. \tag{3}$$

So, once the specific surface area of a solid reactant has been determined, the value of the pore-to-sphere factor can be derived from

$$F = \frac{3}{A\rho_{\text{sol,reac}}} \sum_{i=1}^{i=N} \frac{\nu_i}{R_{p,i}}. \tag{4}$$

The value of A can be measured in several ways, including mercury porosimetry. Consequently, a single mercury porosigram is sufficient to determine the grain-size distribution.

Once the initial sizes of the grains are known, the conversion rate of the grains can be calculated by means of the shrinking-core model first proposed by Yagi and Kunii (1955). According to this model the conversion rate of grains belonging to size class i is given by

$$\frac{\partial X_i}{\partial t} = \frac{3K_{c,i}}{\left[\frac{1}{(1-X_i)^{2/3}}\right] + \psi_i\left[\frac{1}{(1-X_i)^{1/3}} - \frac{1}{(1+KX_i)^{1/3}}\right]} \quad \text{for } X_i < X_{\max,i}$$

$$\frac{\partial X_i}{\partial t} = 0 \quad \text{for } X_i \geq X_{\max,i} \tag{5}$$

where $X_{\max,i}$ represents the maximum attainable conversion of grains belonging to size class i, taking possible pore plugging into account. Whether or not pore plugging occurs depends on the available pore volume around the expanding grains. In our model, we assume that $V_{p,i}$ represents the volume available for grains of size class i to expand. We also assume that the access to these grains is not disturbed when grains of other size classes reach maximum conversion. The value of $X_{\max,i}$ is therefore calculated from

$$X_{\max,i} = \frac{\rho_{\text{sol,reac}} V_{p,i}}{K\nu_i} \quad (\text{if } < 1, \text{ else } X_{\max,i} = 1). \tag{6}$$

Parameter K represents the expansion factor and is a measure for the expansion of grains due to reaction. When assuming that no severe sintering occurs, the relationship between the radius of a grain of size class i, R_{gi}, and its extent of conversion is given by

$$R_{g,i} = (1+KX_i)^{1/3} R_{o,i}, \tag{7}$$

where the expansion factor is defined as

$$K = N_o\left(V_{\text{sol,prod}} - V_{\text{sol,reac}}\right), \tag{8}$$

where $V_{\text{sol,prod}}$ and $V_{\text{sol,reac}}$ represent the molar volume of the solid product (2.76×10^{-5} $\text{m}^3\cdot\text{mol}^{-1}$ for CaS) and the solid reactant (1.68×10^{-5} $\text{m}^3\cdot\text{mol}^{-1}$ for CaO), respectively. Parameter N_o represents the initial concentration of the solid reactant in the grains, and depends on the CaO content (i.e., purity) of the calcined limestone. When it is assumed that the density of any impurities is equal to that of CaO (3,300 $\text{kg}\cdot\text{m}^{-3}$), one obtains

$$N_o = \frac{pur}{V_{\text{sol,reac}}}. \tag{9}$$

The dimensionless parameter ψ_i is defined as

$$\psi_i = \frac{R_{o,i}k_c}{D_s}. \tag{10}$$

When $\psi_i \ll 1$, the chemical reaction is rate controlling, whereas product layer diffusion is limiting when $\psi_i \gg 1$. At intermediate values both chemical reaction and product-layer diffusion affect the rate of conversion.

The overall reaction rate constant $K_{c,i}$ of grains belonging to size class i is defined by

$$K_{c,i} = \frac{k_c C^n}{N_o R_{o,i}}. \tag{11}$$

Finally, the average (local) conversion rate is obtained by summarizing the (local) conversion rates of the grains from the different size classes:

$$\frac{\partial X_p}{\partial t} = \sum_{i=1}^{i=N} \nu_i \frac{\partial X_i}{\partial t}. \tag{12}$$

It has previously been shown by Heesink et al. (1993) that the GSD model, as described earlier, is able to predict both sulfidation and sulfation behavior of multiple calcined limestone batches having different internal structures, provided that reaction takes place in the kinetically controlled regime. Below, we will extend this model to obtain the CPGSD model, which is able to predict conversion behavior under all conditions, including those where internal and/or external mass-transfer limitation occurs.

Transport of H_2S through a calcined limestone particle

As the concentration of H_2S in coal gas is relatively low, transport inside the particles may be described according to Fick's law. Since the calcined limestone particles are bidisperse, the random pore model of Wakao and Smith (1962) is an accurate tool for calculating effective diffusivity:

$$D_e = \epsilon_m^2 D_m + \epsilon_\mu^2 D_\mu + \frac{4\epsilon_m(1-\epsilon_m)}{\frac{1}{D_m} + \frac{(1-\epsilon_m)^2}{\epsilon_\mu^2}\frac{1}{D_\mu}}. \tag{13}$$

Macroporosity (ϵ_m) can be determined from a mercury porosigram of the calcined limestone and typically varies between 2 and 20 vol. % (Hartman et al., 1978). It barely changes upon sulfidation. However, due to grain expansion, the (local) microporosity will diminish:

$$\epsilon_\mu(X_p) = (1-\epsilon_m) - (1-\epsilon_o)(1+KX_p). \qquad (14)$$

The total (local) porosity of a reacting particle is obtained by addition of micro- and macroporosity:

$$\epsilon(X_p) = \epsilon_m + \epsilon_\mu(X_p). \qquad (15)$$

Macropore diffusivity is calculated according to the Wilke-equation, which is accurate for dilute gases. Diffusivity inside the micropore zones is calculated according to the dusty-gas approach, regarding the grains as gaseous molecules that are fixed in space (see, e.g., Wesselingh and Krishna, 1990):

$$D_\mu = \frac{1}{\sum_{j=2}^{j=M} \frac{y_j}{D_{1j}} + \sum_{k=1}^{k=N} \frac{z_k}{D_{1k}}}. \qquad (16)$$

The second term in the denominator of Eq. 16 reflects the friction between H_2S and the grains. The parameter z_k represents the "mole fraction" of grains of size class k in the micropore zones and is given by

$$z_k = \left[\frac{\nu_k \frac{(1-\epsilon_o)}{(1-\epsilon_m)}}{\frac{4}{3}\pi R_{o,k}^3} \right] \Bigg/ \left[\frac{N_A P \frac{\epsilon_\mu}{(1-\epsilon_m)}}{RT} \right]. \qquad (17)$$

The binary diffusion coefficient of H_2S and grains of size class k is calculated according to the kinetic-gas theory by regarding the grains as gaseous molecules with an infinitely large molecular weight and an infinitely large radius. This yields

$$D_{1k} = \frac{2^{5/2}}{\pi^{3/2}} \frac{(RT)^{3/2}}{4R_{g,k}^2 N_A P M_1^{1/2}}. \qquad (18)$$

By combining Eqs. 7, 14, 17, and 18, one obtains

$$\frac{z_k}{D_{1k}} = \frac{3\pi^{1/2}\nu_k(1-\epsilon_o)M_1^{1/2}(1+KX_k)^{2/3}}{2^{5/2}(RT)^{1/2}R_{o,k}\left[(1-\epsilon_m)-(1-\epsilon_o)(1+KX_p)\right]}. \qquad (19)$$

In many models the dimensionless diffusivity D ($= D_e/D_{eo}$) is calculated by the relation proposed by Wen (1968):

$$D = \left[\frac{\epsilon}{\epsilon_o} \right]^\beta. \qquad (20)$$

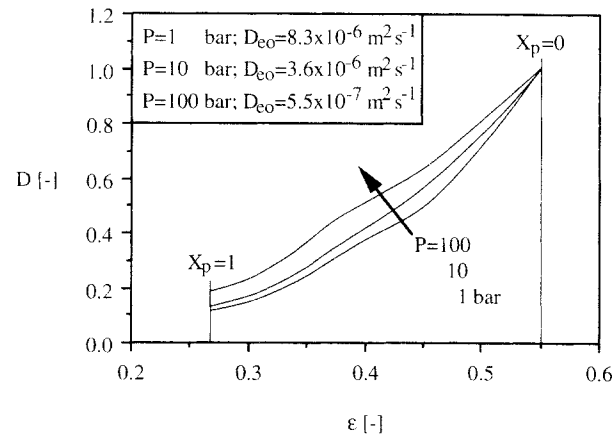

Figure 3. Dimensionless diffusivity against particle porosity for the sulfidation of calcined Wülfrath limestone with H_2S; calculations refer to the porosigram of Figure 2.

$N = 5$; $K = 0.625$; $T = 700°C$; $\epsilon_m = 0.05$; $D_m = 2 \times 10^{-4}$ m^2 s^{-1}.

In the literature β-values of 1 (Satterfield, 1970), 2 (Simons and Garman, 1986), and 3 (Bliek, 1984) have been reported. In Figure 3 the dimensionless diffusivity, as calculated for the microstructure represented by Figure 2, is plotted against particle porosity. The obtained β-values vary between about 2 at a pressure of 100 bar and about 3 at a pressure of 1 bar, and thus fit in the range mentioned in the literature.

In our model we neglected the contribution of surface diffusion to the intraparticle transport of H_2S. It can be shown that surface diffusion indeed plays a minor role by making use of the findings of Heesink and van Swaaij (1995b), who examined the adsorption of H_2S on sulfided limestone, and those of Sladek et al. (1974), who examined the dependency of surface diffusion on the heat of adsorption.

Mass balances

In order to determine the conversion behavior of a single limestone particle, the differential mass balances for both H_2S and CaO have to be solved. In deriving these balances, it is assumed that the sulfidation reaction is irreversible, which is reasonable at temperatures below 800°C and H_2O contents below 3 vol. %. It is further assumed that the particles do not change in size due to grain expansion or attrition. Finally, the particles are assumed to remain isothermal during sulfidation, which can be verified using the criteria given by Froment and Bischoff (1990).

By proper choice of dimensionless parameters, the following mathematical expressions are obtained:

H_2S

$$\frac{\partial(ce)}{\partial\theta} = \frac{1}{\xi^2}\frac{\partial}{\partial\xi}\left[D\xi^2 \frac{\partial c}{\partial\xi} \right] - \phi_o^2 c^n \sum_{i=1}^{i=N} \left[\frac{\nu_i}{r_{o,i}} \kappa(X_i) \right]. \qquad (21)$$

CaO:

$$\frac{\partial X_p}{\partial\theta} = \phi_o^2 \lambda c^n \sum_{i=1}^{i=N} \left[\frac{\nu_i}{r_{o,i}} \kappa(X_i) \right], \qquad (22)$$

with boundary conditions:

$$\theta = 0: \quad C(\xi) = 0 \quad e(\xi) = 1 \quad X_i(\xi) = 0 \quad \text{for } i = 1, \ldots, N$$

$$\xi = 0: \quad \frac{\partial c(\theta)}{\partial \xi} = 0 \quad \frac{\partial X_i(\theta)}{\partial \xi} = 0 \quad \text{for } i = 1, \ldots, N$$

$$\xi = 1: \quad D\frac{\partial c}{\partial \xi} = Bi(1-c) \tag{23}$$

The applied dimensionless numbers are defined as follows:

$$\xi = \frac{r}{R_p} \quad \theta = \frac{D_{eo}t}{R_p^2 \epsilon_o} \quad c = \frac{C}{C_{\text{bulk}}} \quad e = \frac{\epsilon}{\epsilon_o} \quad D = \frac{D_e}{D_{eo}}$$

$$\phi_o = R_p\sqrt{\frac{k_o C_{\text{bulk}}^{n-1}}{D_{eo}}} \quad \lambda = \frac{\epsilon_o C_{\text{bulk}}}{(1-\epsilon_o)N_o} \quad r_{o,i} = \frac{R_{o,i}}{R_{o,\text{avg}}}$$

$$Bi = \frac{k_g R_p}{D_{eo}}$$

$$\kappa(X_i) = \frac{1}{\left[\frac{1}{(1-X_i)^{2/3}} + r_{o,i}\psi\left[\frac{1}{(1-X_i)^{1/3}} - \frac{1}{(1+KX_i)^{1/3}}\right]\right]}$$

$$\psi = \frac{k_c R_{o,\text{avg}}}{D_s}, \tag{24}$$

where R_p, k_g, and C_{bulk} represent the particle radius, the mass-transfer coefficient, and the concentration of H_2S in the surrounding gaseous bulk (which is assumed not to vary with time), respectively. Parameter ϕ_o represents the well-known Thiele modulus, which is based on the initial effective diffusivity D_{eo} and the initial kinetic constant, which is defined as

$$k_o = \frac{3k_c(1-\epsilon_o)}{R_{o,\text{avg}}}, \tag{25}$$

where $R_{o,\text{avg}}$ represents the average initial grain radius, namely, the radius that would be calculated on the basis of the specific surface area while assuming that all grains have an equal radius:

$$R_{o,\text{avg}} = \frac{3}{\rho_{\text{sol,reac}} A} = \frac{1}{\sum_{i=1}^{i=N}\left[\frac{\nu_i}{R_{o,i}}\right]}. \tag{26}$$

Equations 13 to 19, together with Eqs. 21 to 26, form the complete set of equations for the CPGSD model. This set can be solved by numerical calculation after values for the limestone related parameters R_p, pur, ϵ_o, ϵ_m, A, ν_i, and $r_{o,i}$ (the latter four to be determined by mercury porosimetry), the kinetic parameters k_c, D_s, and n (to be determined by thermogravimetric analysis), and the process-related parameters P, T, C_{bulk}, and k_g have been inserted. Notice that no fitting parameters are included.

Definition of the utilization factor

In order to obtain a means to apply the results obtained with the CPGSD model in reactor modeling, a new utilization factor is defined. This factor expresses the ratio of the actual reactivity of a particle and the reactivity that this particle would show if all grains would initially have a radius $R_{o,\text{avg}}$ and no mass-transfer limitation would occur in the surrounding gas phase, in the pores, or in the product layer ($\psi \approx 0$). In the latter case, the particle would be converted homogeneously, that is, all grains inside a particle would show the same extent of conversion at all stages of sulfidation.

The actual reactivity of a particle is given by

$$\text{Actual reactivity} = \int_{r=0}^{r=R_p}\left[4\pi r^2 k_o C^n(r) \sum_{i=1}^{i=N}\left[\frac{\nu_i}{r_{o,i}}\kappa(X_i(r))\right]dr\right]. \tag{27a}$$

The reactivity in the case of homogeneous conversion behavior would be

$$\text{Homogeneous reactivity} = \frac{4}{3}\pi R_p^3 k_o (1-X_p)^{2/3} C_{\text{bulk}}^n. \tag{27b}$$

Division of Eq. 27a by Eq. 27b and substitution of the dimensionless parameters ξ and c yields the definition of the utilization factor H:

$$H = \frac{3\int_{\xi=0}^{\xi=1}\left[\xi^2 c^n \sum_{i=1}^{i=N}\left[\frac{\nu_i}{r_{o,i}}\kappa(X_i)\right]d\xi\right]}{(1-X_p)^{2/3}}. \tag{28}$$

The actual reactivity of a particle can now be calculated from:

$$\text{Actual reactivity} = H\frac{4}{3}\pi R_p^3 k_o (1-X_p)^{2/3} C_{\text{bulk}}^n. \tag{29}$$

Application of the utilization factor H thus offers a means to correct reactivity for the effects of (1) grain size distribution, (2) external mass-transfer limitation, (3) pore-diffusion limitation, and (4) product layer diffusion limitation.

The value of H is delivered by the CPGSD model. It will be shown below that it is possible to express H as a function of X_p and relevant process parameters in an explicit way.

Numerical-solution method

The set of nonlinear partial differential equations was solved by the finite difference solution method, using the two-dimensional discretization scheme developed by Baker and Oliphant (1960). The number of grain-size classes was fixed at 5. The applied numerical solution method was checked by comparing the particle-conversion behavior predicted by the model with the behavior that can analytically be calculated for the simple case of a gas–solid reaction, which is first order in the gaseous reactant, zeroth order in the solid reactant, and takes place at constant particle diffusivity while

the Bi number is infinite (Ishida and Wen, 1968). The agreement between numerically and analytically obtained solutions was satisfactory at all applied ϕ_o numbers.

Experimental Verification

The CPGSD model was experimentally verified by sulfiding two batches of calcined limestone in an atmospheric thermogravimetric analyzer (type Setaram TG-85). Table 1 shows the composition of the applied limestone from the German quarry at Wülfrath. One batch consisted of particles having a diameter ranging from 150 μm to 210 μm. The diameter of the particles from the other batch varied between 850μm and 900 μm. Both batches were first calcined at 850°C while purging with helium. Calcination was stopped after about 30 min when no decrease in sample weight was observed anymore. About 500 mg of each batch was used for mercury porosimetry (a Carlo Erba Strumentazione porosimeter, type DRU model 204 was applied). The resulting porosigrams were almost identical, showing surface areas of 18.0 and 18.1 m^2g^{-1} and average pore radii of 33.6 nm and 31.5 nm for the respective batches. The corresponding pore-to-sphere factors were calculated to be 1.56 and 1.53, respectively.

About 5 mg of each calcined batch was sulfided in the TGA at 700°C applying a gas mixture consisting of 2 vol % H_2S, 4 vol % H_2, and balance He. The obtained conversion vs. time curves were simulated with the CPGSD model. The values of the reaction rate constant k_c and the reaction order n, which are needed for the calculations, were taken from Heesink and Van Swaaij (1995a):

$$k_c = 5{,}946 \exp\left(-\frac{154{,}000}{RT}\right)$$

$$\Rightarrow k_{c,700°C} = 3.2 \times 10^{-5}\ \text{mol}^{0.5} \cdot \text{m}^{-0.5} \cdot \text{s}^{-1}$$

$$n = 0.5. \qquad (30)$$

Since Heesink and Van Swaaij (1995a) have shown that the sulfidation of calcined limestone with H_2S is not limited by product layer diffusion, an extremely high D_s-value of 10^{12} $\text{mol}^{0.5} \cdot \text{m}^{0.5} \cdot \text{s}^{-1}$ was inserted, resulting in ψ_t-values of typically 10^{-24}. Initial porosity ϵ_o and macroporosity ϵ_m were derived from the mercury porosigrams of the calcined limestone batches, and were determined at 0.55 and 0.05, respectively, for both batches.

Table 1. Chemical Composition of the Applied Wülfrath Limestone Before and After Calcination (in wt. %)

Component	Calcination	
	Before	After*
$CaCO_3$	97.20	—
$MgCO_3$	0.90	—
CaO	—	95.90
MgO	—	0.76
Si	0.54	0.95
Fe	0.09	0.16
Al	0.06	0.11
S	0.02	0.04
K	0.02	0.04
Sr	0.02	0.04

*Calculated from the composition before calcination, assuming complete calcination.

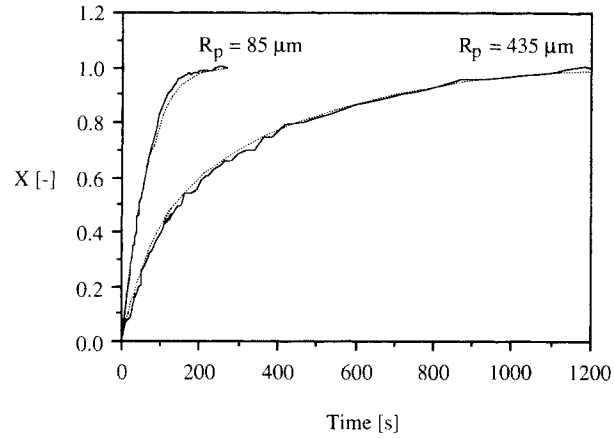

Figure 4. Measured (solid lines) and calculated (dotted lines) conversions vs. time behavior of calcined Wülfrath limestone particles of different size.

Sulfidation performed at 700°C applying a gas mixture of 2 vol % H_2S, 4 vol % H_2, and balance N_2.

Figure 4 shows good agreement between the measured and the simulated conversion vs. time curves for both batches. We therefore conclude that the CPGSD model is quite well able to describe the sulfidation behavior of calcined limestone particles, also when pore-diffusion limitation occurs, as in the case of the particles with a radius of 435 μm.

Analysis

The sulfidation behavior of a given batch of calcined limestone only depends on the independent parameters ϕ_o, Bi, λ, ψ, and n, which in their turn depend on limestone characteristics, operating conditions, and reactor characteristics. Calculations were performed to find out how the utilization factor H is influenced by the first two parameters. These highly depend on process conditions. The other parameters are less revelant or may be regarded as constants.

The following set of (standard) values was selected:

$\phi_o = 0.1$ or 10: varied between 0.1 and 50
Bi = 10: varied between 0.01 and 100
$\lambda = 10^{-5}$: not varied
$\psi = 10^{-20}$: not varied
n = 0.5: not varied
N = 5: not varied.

The applied values of ϕ_o and Bi cover the full range of limestone characteristics and operating conditions encountered in practice. Realistic values of λ may vary from 10^{-5} to 10^{-4}. At values that low, the pseudo-steady-state assumption is valid (see, e.g., Froment and Bischoff, 1990) and the precise value of λ is not relevant. The fixed values of ψ and n were taken from Heesink and Van Swaaij (1995a), who found that product layer diffusion does not limit the rate of sulfidation ($\psi \ll 1$) and measured a reaction order (n) of 0.5 in H_2S. The number of grain-size classes (N) was fixed at 5, which was previously found to be high enough to include the effects of

grain size distribution on conversion behavior in the kinetically controlled regime (Heesink et al., 1993).

The porosigram of Figure 2 was used as input for the model. From this porosigram $R_{p,i}$ values 21, 30, 40, 53 and 78 nm and corresponding ν_i values of 0.17, 0.35, 0.32, 0.12 and 0.04 were derived. The pore-to-sphere factor was calculated to be 1.56, resulting in an $R_{o,\text{avg}}$ value of 51 nm. Values of 0.55 and 0.05 were inserted for the respective porosities ϵ_o and ϵ_m. For K, a value of 0.625 was taken. Temperature and pressure were fixed at 600°C and 1 bar, respectively. The value of D_m was calculated to be $10^{-4}\cdot\text{m}^2\cdot\text{s}^{-1}$ for a gas mixture containing H_2S and N_2 only.

The influence of ϕ_o

Figure 5 illustrates the influence of ϕ_o on H vs. X_p behavior. At the low ϕ_o value of 0.1, pore-diffusion limitation hardly occurs. Because of the high Bi number of 10, external mass-transfer limitation may also be excluded. Therefore, the dimensionless concentration (c) of H_2S amounts to unity throughout the reacting particle and Eq. 28 can be rewritten as

$$H = \frac{\sum_{i=1}^{i=N}\left[\frac{\nu_i}{r_{o,i}}\kappa(X_i)\right]}{(1-X_p)^{2/3}}. \qquad (31)$$

At the conversion extent of zero [$X_i = X_p = 0$; $\kappa(X_i) = 1$], Eq. 31 yields a value of unity (see also Figure 5). At increasing conversion extents H drops below unity due to the distribution in grain size. As conversion proceeds the smaller grains become fully sulfided and stop reacting. The remaining grains are relatively large and therefore less reactive, resulting in lower H values.

At larger ϕ_o values pore diffusion limitation occurs, resulting in lower H values. However, the decrease in H value as conversion proceeds is less than the decrease observed at low ϕ_o values. In some cases a slight increase in H is even observed, indicating that the average reactivity of a particle decreases faster with conversion than its effective diffusivity, resulting in less pore-diffusion limitation.

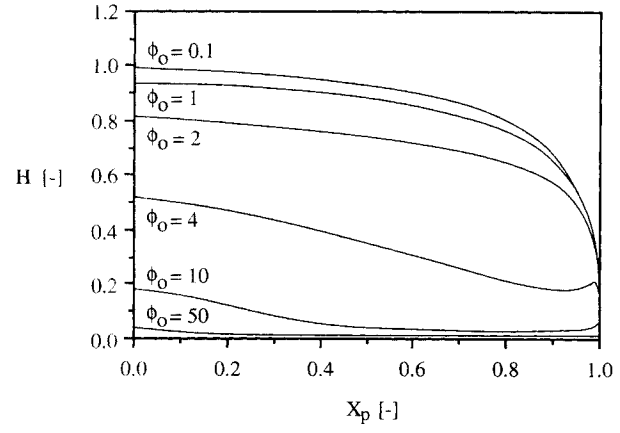

Figure 5. Utilization factor H vs. X_p behavior at different values of ϕ_o.

Bi = 10, $\lambda = 10^{-5}$, $\psi = 10^{-20}$, $n = 0.5$. Calculations based on the porosigram of Figure 2. T = 600°C, P = 1 bar.

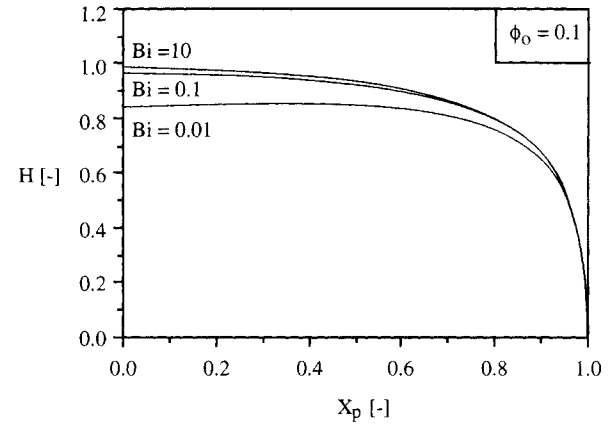

Figure 6. Utilization factor H vs. X_p behavior at different values of Bi.

$\phi_o = 0.1$, $\lambda = 10^{-5}$, $\psi = 10^{-20}$, $n = 0.5$. Calculations based on the porosigram of Figure 2. T = 600°C, P = 1 bar.

Influence of Bi

In Figures 6 and 7 the influence of Bi on H vs. X_p behavior is shown at ϕ_o values of 0.1 and 10, respectively. At a ϕ_o value of 0.1 the value of Bi hardly is of interest. This can be explained by expressing the ratio of the maximum H_2S supply and its maximum consumption in terms of Bi and ϕ_o:

$$\text{max. supply: } k_g 4\pi R_p^2 C_{\text{bulk}}$$

$$\text{max. consumption: } \frac{4}{3}\pi R_p^3 k_o \sum_{i=1}^{i=N}\left[\frac{\nu_i}{r_{o,i}}\kappa(X_i)\right] C_{\text{bulk}}^n, \qquad (32)$$

yielding

$$\frac{\text{max. supply}}{\text{max. consumption}} = \frac{3\,Bi}{\phi_o^2 \sum_{i=1}^{i=N}\left[\frac{\nu_i}{r_{o,i}}\kappa(X_i)\right]}. \qquad (33)$$

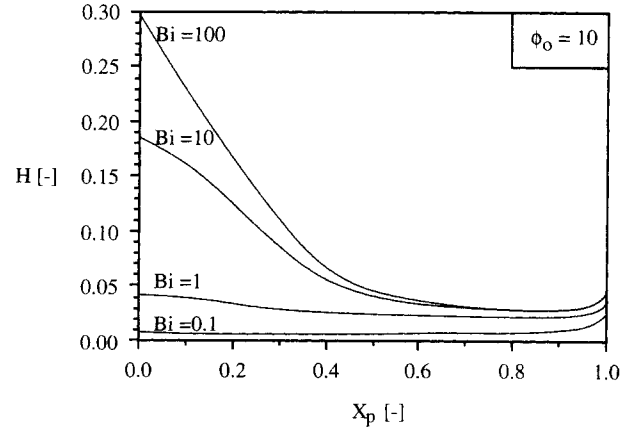

Figure 7. Utilization factor H vs. X_p behavior at different values of Bi.

$\phi_o = 10$, $\lambda = 10^{-5}$, $\psi = 10^{-20}$, $n = 0.5$. Calculations based on the porosigram of Figure 2. T = 600°C, P = 1 bar.

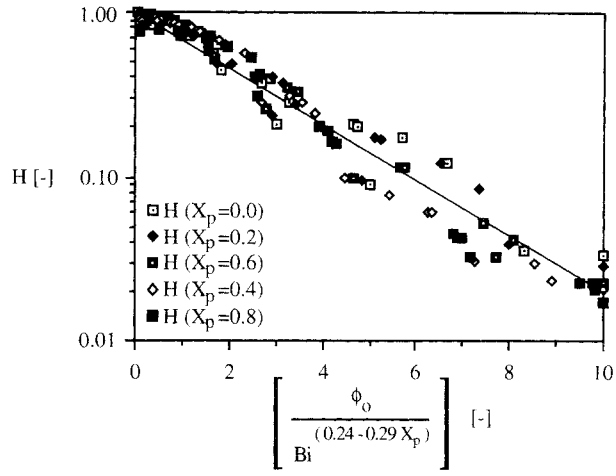

Figure 8. Comparison of *H* values calculated with CPGSD model to values estimated by Eq. 34 (solid line).

Calculations based on the porosigram of Figure 2. $T = 600°C$, $P = 1$ bar.

Large values of this ratio correspond with situations where external mass transfer is not limiting and where the value of Bi is not of interest. This explains the results obtained with the low ϕ_o value of 0.1 (Figure 6). When ϕ_o equals 10, high Bi values are needed to avoid external mass-transfer limitation, as can be seen in Figure 7.

Derivation of a simplified correlation

The calculation results were evaluated to obtain a simplified correlation expressing H as a function of X_p, ϕ_o, and Bi:

$$H = 10^{[(-0.17\phi_o)/(\mathrm{Bi}^{[0.24-0.29X_p]})]}. \qquad (34)$$

Figure 8 shows reasonable agreement between H values calculated by the model and those obtained by making use of Eq. 34.

Application to Reactor Modeling

Unlike many other models that describe the conversion behavior of a single particle undergoing reaction, the CPGSD model can easily be inserted in reactor models. In general, the following strategy may be applied. First, the intrinsic kinetics of the involved gas–solid reaction are to be determined, for example, by thermogravimetric analysis. The limiting step in the reaction mechanism, being either chemical reaction at the surface of the unreacted core or product layer diffusion, is determined with the help of the GSD model. Secondly, the internal structure of the unconverted porous particles is characterized to determine the size distribution of the grains, for example, by mercury porosimetry. Then, with this information available, the CPGSD model is exploited to obtain the utilization factor H as an explicit function of the dimensionless parameters Bi, ϕ_o, λ, and ψ. An example of such a function is given by Eq. 34. Finally, actual reactivity is calculated as a function of X_p and H with the help of Eq. 29.

The value of X_p, which may change with time and place, is obtained by solving the mass balance over the reactor or parts thereof. Because H is a function of ϕ_o and λ, which in their turn are a function of C_{bulk}, H should be calculated on the basis of the actual value of C_{bulk}, which is not necessarily constant. For example, in a fluidized bed particles move randomly through the bed, encountering high gas concentrations in the bottom part of the bed and lower concentrations in the upper part of the bed. Though the CPGSD model assumes that the value of C_{bulk} remains constant during conversion, errors made due to variations in C_{bulk} are relatively small.

Example

In order to demonstrate the applicability of the strategy described earlier, the H-factor concept was incorporated into an existing reactor model that predicts the H_2S capture by a bubbling fluidized bed of calcined limestone particles. This model is based on the two-phase model developed by Werther (1978). See Heesink and Van Swaaij (1996) for a detailed description of the hydrodynamic features of the model.

The reactor model, with the H-factor concept incorporated, was verified experimentally by measuring the breakthrough of H_2S for a small bed of calcined limestone particles. First, a batch of 350 g limestone particles from the German quarry in Wülfrath, with diameters ranging from 0.5 mm to 1.4 mm, was calcined by heating to 850°C while purging with nitrogen. Table 1 shows the composition of these particles, both before and after calcination. About 1 g of the calcined material was taken for mercury porosimetry. The resulting porosigram is shown by Figure 2. After the temperature of the bed had been adjusted to 600°C, a gas mixture containing 2 vol % H_2S, 4 vol % H_2, and balance N_2 was led through the reactor. Sulfidation was carried out at atmospheric pressure. The sulfidation conditions and reactor characteristics are summarized in Table 2. The breakthrough of H_2S was measured by combusting a small fraction of the effluent gas and on-line infrared analysis was used to measure the SO_2 content of the flue-gas stream produced.

Breakthrough was also simulated with the reactor model. While doing so, the reactivity of the dense phase inside the reactor was calculated according to

$$R_{\mathrm{dense}} = (1 - \epsilon_{\mathrm{dense}})Hk_o(1 - X_p)^{2/3}C^n_{\mathrm{dense}}. \qquad (35)$$

The reaction rate constant k_o was obtained from Eq. 25. Equation 30 was used to calculate k_c at 600°C, yielding a

Table 2. Experimental Conditions During the Sulfidation of Calcined Wülfrath Limestone in the Fluidized-Bed Reactor

Temperature	600°C
Pressure	1 bar
Static-bed height	0.05 m
Gas composition at inlet	2 vol % H_2S, 4 vol % H_2; balance N_2
Superficial gas velocity	0.63 $m \cdot s^{-1}$
Minimum fluidization velocity	0.13 $m \cdot s^{-1}$
Sauter diameter of particles	7.4×10^{-4} m
Reaction order in H_2S	0.5
Reactor diameter	0.07 m
Number of orifices	140
Orifice diameter	6×10^{-4} m

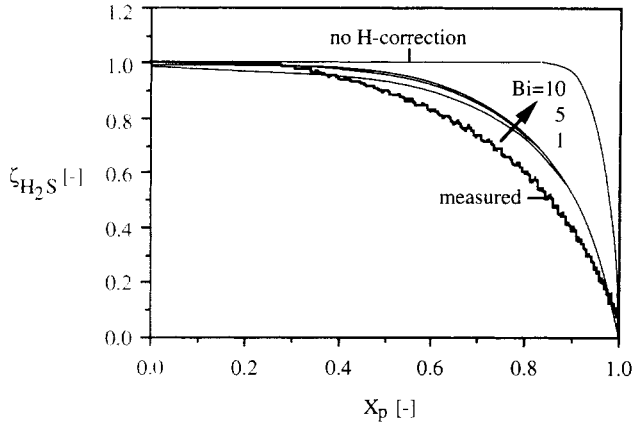

Figure 9. Measured and predicted H_2S capture by a fluidized bed of calcined Wülfrath limestone as a function of particle conversion extent.

See Table 2 for experimental conditions.

value of 3.6×10^{-6} $mol^{0.5}\cdot m^{-0.5}\cdot s^{-1}$. From the porosigram depicted in Figure 2, $R_{o,avg}$ was determined at 51 nm. The value of ϕ_o, to be inserted into Eq. 34, was calculated from Eq. 24 while substituting C_{dense} for C_{bulk}. At a typical H_2S concentration of 1 vol. %, the value of ϕ_o would amount to about 4, resulting in an H value of 0.28 at a particle-conversion extent of 0.5 and Bi numbers of 1 or higher.

In Figure 9 both measured and simulated H_2S capture have been plotted as a function of particle conversion extent, which is assumed to be equal for all particles in the bed. Simulations have been performed for different values of Bi. The value of Bi seems to be irrelevant at values of unity or higher. When applying the relationship, which Prins et al. (1987) derived for mass transfer toward fluidized particles, a value of 30 is obtained. When the H-factor concept is not applied and no other corrections are made for mass-transfer limitation and grain-size distribution, predicted capture is much too high, especially at high particle-conversion extents. Although some difference remains between predicted and measured behavior, which is most probably caused by inaccuracies in the description of the complex hydrodynamics in the applied reactor, much better agreement is obtained when the H-factor concept is applied.

Conclusion

A combined pore- and grain-size distribution model has been developed to simulate the sulfidation of a single calcined limestone particle. Although the model makes no use of fitting parameters, it has been shown to perform well. The model delivers the value of a newly defined utilization factor H, which represents the ratio of actual particle reactivity and the reactivity that would be observed when a particle is converted in a homogeneous way and in the absence of product-layer diffusion limitation. The use of the H-factor concept in reactor modeling offers a simple tool to correct particle reactivity for (1) grain-size distribution, (2) external mass-transfer limitation, (3) internal mass-transfer limitation, and (4) product layer diffusion limitation.

Under realistic sulfidation conditions, H mainly depends on the initial microstructure of the calcined limestone particle, the sulfidation extent X_p of the particle, and the process-related dimensionless numbers ϕ_o and Bi. For a single batch of calcined limestone an explicit expression has been derived that delivers the value of H as a function of X_p, ϕ_o, and Bi. The applicability of this expression in reactor modeling has been demonstrated.

Acknowledgments

This investigation was supported by the Directorate-General XII of the European Communities and TNO-MEP and NOVEM B.V. of The Netherlands. The authors also acknowledge J. A. M. Kuipers for his assistance in the mathematical field, and M. F. B. Koster and J. Nijmeijer for their assistance in the experimental work.

Notation

Bi = Biot number ($= k_g R_p D_{eo}^{-1}$)
C = (local) concentration of H_2S, $mol\cdot m^{-3}$
c = concentration of H_2S ($= C\ C_{bulk}^{-1}$)
D_m = diffusivity inside macropores, $m^2\cdot s^{-1}$
D_{1j} = binary diffusion coefficient of H_2S and component j, $m^2\cdot s^{-1}$
e = dimensionless porosity ($= \epsilon\ \epsilon_o^{-1}$)
k_c = reaction-rate constant, $mol^{1-n}\cdot m^{3n-2}\cdot s^{-1}$
k_o = initial volumetric reaction-rate constant, $mol^{1-n}\cdot m^{3n-3}\cdot s^{-1}$
M = number of gaseous components
M_1 = molecular weight of H_2S, $kg\cdot mol^{-1}$
n = reaction order in H_2S
N_A = Avogadro number ($= 6.023\times10^{23}$), mol^{-1}
P = (total) pressure, Pa
pur = initial weight fraction of CaO in grains (purity)
R = gas constant, $J\cdot mol^{-1}\cdot K^{-1}$
$R_{p,i}$ = radius of pores of size class i, m
$r_{o,i}$ = dimensionless radius of grains of size class i ($= R_{o,i}R_{o,avg}$)
T = temperature, K
t = time, s
X_p = (local) conversion of particle as a whole
y_j = mole fraction of component j in gas mixture
ϵ = porosity of particle ($= \epsilon_m + \epsilon_\mu$)
ϵ_{dense} = interparticle porosity of the dense phase in a fluidized-bed reactor
ϵ_o = initial porosity of particle
ζ_{H_2S} = fraction of H_2S captured by the fluidized bed
θ = dimensionless time
$\kappa(X_i)$ = dimensionless reactivity of grains of size class i
λ = ratio of H_2S and CaO concentrations
ξ = dimensionless radius
$\rho_{sol,reac}$ = density of CaO, $kg\cdot m^{-3}$
τ = tortuosity of calcined limestone particle
ψ = ratio of the rates of chemical reaction and product-layer diffusion, referring to average grain size
ψ_i = ratio of the rates of reaction and product-layer diffusion, referring to grains from size class i

Literature Cited

Allen, D., and A. N. Hayhurst, "The Kinetics of the Reaction Between Calcium Oxide and Hydrogen Sulfide at the Temperatures of Fluidized Bed Combustors," *Proc. Symp. (Int.) on Combustion*, Combust. Inst., Pittsburgh, p. 935 (1990).

Alvfors, P., and G. Svedberg, "Modeling of the Simultaneous Calcination, Sintering, and Sulfation of Limestone and Dolomite," *Chem. Eng. Sci.*, **47**, 1903 (1992).

Baker, G. A., and T. A. Oliphant, "An Implicit, Numerical Method for Solving the Two-Dimensional Heat Equation," *Q. Appl. Math.*, **17**, 361 (1960).

Bhatia, S. K., and D. D. Perlmutter, "A Random Pore Model for Fluid-Solid Reactions. II: Diffusion and Transport Effects," *AIChE J.*, **27**, 247 (1981).
Bliek, A., "Mathematical Modeling of a Cocurrent Fixed Bed Coal Gasifier," PhD Thesis, Twente Univ. of Technology, Enschede, The Netherlands (1984).
Borgwardt, R. H., and R. D. Harvey, "Properties of Carbonate Rocks Related to SO_2 Reactivity," *Environ. Sci. Technol.*, **6**, 350 (1972).
Brem, G., "Mathematical Modeling of Coal Conversion Processes; With Application to Atmospheric Fluidized Bed Combustion," PhD Thesis, Twente Univ. of Technology, Enschede, The Netherlands (1990).
Dam-Johansen, K., P. F. B. Hansen, and K. Østergaard, "High-Temperature Reaction Between Sulfur Dioxide and Limestone: III. A Grain-Micrograin Model and Its Verification," *Chem. Eng. Sci.*, **46**, 847 (1991).
Efthimiadis, E. A., and S. V. Sotirchos, "Reactivity Evolution During Sulfidation of Porous Zinc Oxide," *Chem. Eng. Sci.*, **48**, 829 (1993a).
Efthimiadis, E. A., and S. V. Sotirchos, "A Partially Overlapping Grain Model for Gas-Solid Reactions," *Chem. Eng. Sci.*, **48**, 1201 (1993b).
Fenouil, L. A., and S. Lynn, "Study of Calcium-Based Sorbents for High-Temperature H_2S Removal. 1. Kinetics of H_2S Sorption by Uncalcined Limestone," *Ind. Eng. Chem. Res.*, **34**, 2324 (1995a).
Fenouil, L. A., and S. Lynn, "Study of Calcium-Based Sorbents for High-Temperature H_2S Removal. 2. Kinetics of H_2S Sorption by Calcined Limestone," *Ind. Eng. Chem. Res.*, **34**, 2334 (1995b).
Froment, G. F., and K. B. Bischoff, *Chemical Reactor Analysis and Design*, 2nd ed., Wiley, New York (1990).
Hartman, M., and W. R. Coughlin, "Reaction of Sulfur Dioxide with Limestone and the Grain Model," *AIChE J.*, **22**, 490 (1976).
Hartman, M., J. Pata, and W. R. Coughlin, "Influence of Porosity of Calcium Carbonates on their Reactivity with Sulfur Dioxide," *Ind. Eng. Chem. Proc. Des. Dev.*, **17**, 411 (1978).
Heesink, A. B. M., W. Prins, and W. P. M. Van Swaaij, "A Grain Size Distribution Model for Non-Catalytic Gas-Solid Reactions," *Chem. Eng. J.*, **53**, 25 (1993).
Heesink, A. B. M., and W. P. M. Van Swaaij, "The Sulfidation of Calcined Limestone with Hydrogen Sulfide and Carbonyl Sulfide," *Chem. Eng. Sci.*, **50**, 2983 (1995a).
Heesink, A. B. M., and W. P. M. Van Swaaij, "The Adsorption of H_2S on Sulfided Limestone," *Chem. Eng. Sci.*, **50**, 3651 (1995b).
Heesink, A. B. M., and W. P. M. Van Swaaij, "The Desulfurization of Simulated Coal Gas with Calcareous Sorbents in a Small Bubbling Fluidized Bed Absorber," *High Temperature Gas Cleaning*, E. Schmidt, P. Gäng, T. Pilz, and A. Dittler, eds., Institut für Mechanische Verfahrenstechnik und Mechanik der Universität Karlsruhe, Germany (1996).
Illerup, J. B., K. Dam-Johansen, and J. E. Johnsson, "Hydrogen Sulfide Retention on Limestone at High Temperature and High Pressure," *Gas Cleaning at High Temperatures*, R. Clift and J. P. K. Seville, eds., Blackie, Glasgow, p. 492 (1993).
Ishida, M., and C. Y. Wen, "Comparison of Kinetic and Diffusional Models for Solid-Gas Reactions," *AIChE J.*, **14**, 311 (1968).
Lew, S., A. F. Sarofim, and F. Stephanopoulos, "Modeling of the Sulfidation of Zinc-Titanium Oxide Sorbents with Hydrogen Sulfide," *AIChE J.*, **38**, 1161 (1992).
Lin, W., "Interactions Between SO_2 and NO_x Emissions in Fluidized Bed Combustion of Coal," PhD Thesis, Technical University of Delft, Delft, The Netherlands (1994).
Nguyen, Q. T., and A. P. Watkinson, "Sulfur Capture During Gasification of Oil Sand Cokes," *Can. J. Chem. Eng.*, **71**, 401 (1993).
Prins, W., T. P. Casteleijn, W. Draijer, and W. P. M. van Swaaij, "Mass-Transfer in Gas-Fluidized Beds: Measurements of Actual Driving Forces," *Chem. Eng. Sci.*, **40**, 481 (1985).
Ramachandran, P. A., and J. M. Smith, "A Single-Pore Model for Gas-Solid Non-Catalytic Reactions," *AIChE J.*, **23**, 353 (1977).
Ranade, P. V., and D. P. Harrison, "The Variable Property Grain Model Applied to the Zinc Oxide–Hydrogen Sulfide Reaction," *Chem. Eng. Sci.*, **36**, 1079 (1981).
Satterfield, C. N., *Mass Transfer in Heterogeneous Catalysis*, MIT Press, Cambridge (1970).
Schouten, J. C., and C. M. Van den Bleek, "The D.U.T. SURE Model: A Simple Approach in FBC Sulfur Retention Modeling," *Proc. Int. Conf. on Fluidized Bed Combustion*, Vol. 2, Boston, p. 749 (1987).
Simons, G. A., and A. R. Garman, "Small Pore Closure and the Deactivation of the Limestone Sulfation Reaction," *AIChE J.*, **32**, 1491 (1986).
Sladek, K. J., E. R. Gilliland, and R. F. Baddour, "Diffusion on Surfaces: II. Correlation of Diffusivities of Physically and Chemically Adsorbed Species," *Ind. Eng. Chem. Fundam.*, **13**, 100 (1974).
Szekely, J., and M. Propster, "A Structural Model for Gas-Solid Reactions with a Moving Boundary: VI. The Effect of Grain Size Distribution on the Conversion of Porous Solids," *Chem. Eng. Sci.*, **30**, 1049 (1975).
Szekely, J., and J. W. Evans, "A Structural Model for Gas-Solid Reactions with a Moving Boundary," *Chem. Eng. Sci.*, **25**, 1091 (1970).
Wakao, N., and J. M. Smith, "Diffusion in Catalyst Pellets," *Chem. Eng. Sci.*, **17**, 825 (1962).
Wen, C. Y., "Non-Catalytic Heterogeneous Solid Fluid Reaction Models," *Ind. Eng. Chem. Fundam.*, **60**, 34 (1968).
Werther, J., "Mathematische Modellierung von Wirbelschichtreaktoren," *Chem.-Ing.-Tech.*, **50**, 850 (1978).
Wesselingh, J. A., and R. Krishna, *Mass Transfer*, Ellis Horwood, New York, p. 110 (1990).
Yagi, S., and D. Kunii, *Proc. Symp. (Int.) on Combustion*, The Combustion Institute, Pittsburgh, p. 231 (1955).
Zevenhoven, C. A. P., K. P. Yrjas, and M. M. Hupa, "Hydrogen Sulfide Capture by Limestone and Dolomite at Elevated Pressure: 2. Sorbent Particle Conversion Modeling," *Ind. Eng. Chem. Res.*, **35**, 943 (1996).

Manuscript received Aug. 26, 1997, and revision received Mar. 25, 1998.